NeuroImage 262 (2022) 119552

Contents lists available at ScienceDirect

NeuroImage

journal homepage: www.elsevier.com/locate/neuroimage

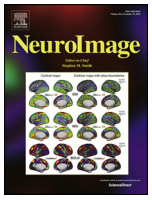

Interrater reliability of deep brain stimulation electrode localizations

Roxanne Lofredi[a,b,*], Cem-Georg Auernig[a], Siobhan Ewert[a], Friederike Irmen[a], Leon A. Steiner[a,b], Ute Scheller[a,c], Bernadette C.M. van Wijk[a,d,e], Simon Oxenford[a], Andrea A. Kühn[a,f,g,h,i], Andreas Horn[a,j,k]

[a] Department of Neurology, Charité-Universitätsmedizin Berlin, Berlin, Germany
[b] Berlin Institute of Health (BIH), Berlin, Germany
[c] Department of Neurology, Universitätsmedizin Göttingen, Göttingen, Germany
[d] Department of Human Movement Sciences, Vrije Universiteit Amsterdam, Amsterdam, The Netherlands
[e] Department of Neurology, Amsterdam University Medical Center, Amsterdam, The Netherlands
[f] Bernstein Center for Computational Neuroscience, Humboldt-Universität, Berlin, Germany
[g] NeuroCure, Exzellenzcluster, Charité-Universitätsmedizin Berlin, Berlin, Germany
[h] DZNE, German center for neurodegenerative diseases, Berlin, Germany
[i] Berlin School of Mind and Brain, Humboldt-Universität zu Berlin
[j] Center for Brain Circuit Therapeutics Department of Neurology Brigham & Women's Hospital, Harvard Medical School
[k] MGH Neurosurgery & Center for Neurotechnology and Neurorecovery (CNTR) at MGH Neurology, Massachusetts General Hospital, Harvard Medical School

ARTICLE INFO

Keywords:
Parkinson's disease
Deep brain stimulation
Subthalamic nucleus
Lead-DBS
Localization

ABSTRACT

Lead-DBS is an open-source, semi-automatized and widely applied software tool facilitating precise localization of deep brain stimulation electrodes both in native as well as in standardized stereotactic space. While automatized preprocessing steps within the toolbox have been tested and validated in previous studies, the interrater reliability in manual refinements of electrode localizations using the tool has not been objectified so far. Here, we investigate the variance introduced in this processing step by different raters when localizing electrodes based on postoperative CT or MRI. Furthermore, we compare the performance of novel trainees that received a structured training and more experienced raters with an expert user. We show that all users yield similar results with an average difference in localizations ranging between 0.52–0.75 mm with 0.07–0.12 mm increases in variability when using postoperative MRI and following normalization to standard space. Our findings may pave the way toward formal training for using Lead-DBS and demonstrate its reliability and ease-of-use for imaging research in the field of deep brain stimulation.

Introduction

Deep brain stimulation (DBS) is an established treatment option for numerous brain disorders, often with a direct correlation between electrode placement and clinical outcomes (Horn, 2019). To investigate this correlation and further explore location-specific DBS-effects in scientific studies, it is crucial to exactly reconstruct electrode placement. The open-source toolbox Lead-DBS was developed with this aim in 2012 by the last author of the present study (Horn and Kühn, 2015a) and has since continuously been optimized by investigators from various institutions (Dembek et al., 2019; Ewert et al., 2018, 2019; Horn et al., 2017; Horn et al., 2019a; Horn and Kühn, 2015b; Husch et al., 2018; Treu et al., 2020). In brief, Lead-DBS facilitates semiautomatic localization based on structural neuroimaging. Postoperative CT or MRI scans containing defined artifacts of the DBS-electrode are co-registered to preoperative anatomical MRI scans. Preoperative MRI scans are used to non-linearly register ('normalize') patient scans to standard stereotactic space for group comparisons. Lead-DBS also allows the estimation of stimulation volumes (Horn et al., 2019a) and the calculation of connectivity profiles from stimulation sites (Horn and Fox, 2020). It was designed with a research focus in mind and leverages group-level statistics to derive at robust conclusions (Treu et al., 2020). While other tools have since been developed with the same aim (for an overview about tool alternatives see Horn et al., 2019a), Lead-DBS has empowered over 200 publications and has been referred to as the most established tool for DBS-electrode localization (Alkemade et al., 2018; Husch et al., 2018; Milchenko et al., 2018) with over 20,000 downloads.

Abbreviations: DBS, Deep Brain Stimulation; PD, Parkinson's disease; STN, subthalamic nucleus.

* Corresponding author at: Department of Neurology - Campus Mitte, Charité Universitätsmedizin Berlin, Charitéplatz 1, 10117 Berlin, Germany.
E-mail address: roxanne.lofredi@charite.de (R. Lofredi).

https://doi.org/10.1016/j.neuroimage.2022.119552.
Received 18 February 2022; Received in revised form 15 July 2022; Accepted 8 August 2022
Available online 16 August 2022.

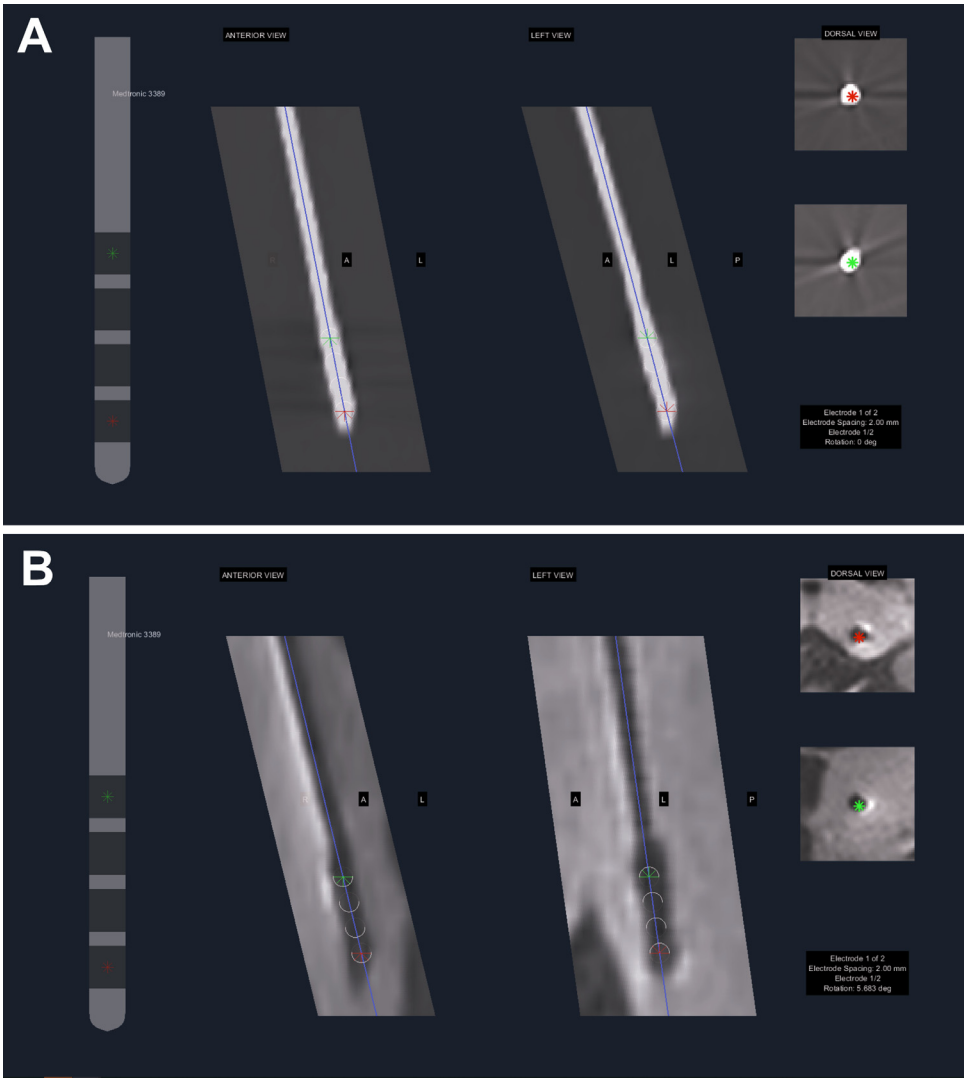

Fig. 1. Examples of electrode models matched onto electrode artifacts visible on post-operative CT (A) and MRI (B) as visualized in Lead-DBS. From left to right: Electrode model (here Medtronic 3389) plotted onto the electrode artifact as visible on two orthogonal planes of a probes eye view of the post-operative CT (A) or MRI (B). The upper- and lowermost contacts of the electrode model are additionally plotted in the axial plane to allow for an optimal adjustment of the pre-localized position of the electrode model in all three axes.

The core process of electrode reconstructions by Lead-DBS can be broken down to four major steps: co-registration, brain shift correction, normalization, and electrode localization. While the former two are comparably trivial, the latter two regularly involve manual refinement and thus introduce serious bias into the process which makes it crucial to assess their precision.

Variance in normalization techniques has been empirically assessed and quantified in previous studies (Ewert et al., 2019; Horn et al., 2019a; Vogel et al., 2020). These led to a default pathway in Lead-DBS that generates results comparable to manual expert segmentation (Ewert et al., 2019) and further manual refinement and control steps have been developed since (Edlow et al., 2019; Oxenford et al., 2021).

In contrast, manual localization of an electrode model within the electrode artifact in postoperative scans, has not been analyzed deliberately yet. This step involves manually aligning an automatically pre-localized electrode model to electrode artifacts visible on CT and MRI. The tool specifically designed in Lead-DBS to manually localize DBS electrodes shows probe-eye sections, i.e., the brain is three-dimensionally resliced orthogonally to the reconstruction (electrode) at any time point. When changing the reconstruction, this view is updated, resulting in a renewed reslicing of the images.

As electrode artifacts have blurred borders, are larger than the actual electrode and differ in presentation across postoperative modalities (see Fig. 1), interrater variance is introduced into the process. This could especially apply to unexperienced users and the postoperative MRI modality, since for postoperative CT, a phantom-validated automated method is included in Lead-DBS, which reliably and precisely pre-localizes electrodes in most cases (Husch et al., 2018). Here, we aimed to assess the interrater variance of novel and more experienced Lead-DBS users within different post-operative modalities as they localized DBS-electrodes in a group of patients that received both post-operative CT and MRI. Novel users received a structured and documented introduction as provided by the regularly held Lead-DBS workshops. We show that DBS-electrode localization using Lead-DBS has a high interrater reliability with an average difference of 0.6 mm across raters, independently of the available post-operative imaging modality.

Methods and materials

Patient cohort and imaging

For this study, we identified 20 Parkinson's disease patients with bilaterally implanted, subthalamic DBS-electrodes (model 3389; Medtronic) in which both post-operative CT and MRI-scans were available from archival data. Post-operative CT-scans had been performed to verify correct electrode placement in 1–7 days following DBS-surgery, while post-operative MRI-scans were realized 3–

12 months after DBS-surgery as part of a study which assessed the DBS-effect on functional connectivity and has been published elsewhere (Horn et al., 2019a). Specifications on image acquisition can be found there. The study was approved by the local ethics committee (EA2/175/21) and carried out in accordance with the Declaration of Helsinki.

Participants and study design

Six raters with varying experience in use of Lead-DBS participated in the present study. One expert rater with several years' experience in the use of Lead-DBS (AH), two raters that participated in earlier Lead-DBS workshops and had since used Lead-DBS to a limited extend for own research projects (FI, BCMvW) as well as three raters without prior experience with Lead-DBS or any other electrode localization software (RL, LAS, US). These novice raters, one medical student and 2 neurology residents with ~1 year experience in DBS programming, were introduced to Lead-DBS by a structured two days' workshop comparable to the Lead-DBS workshops that have regularly been held worldwide (All screencasts from a 2018 workshop in Shanghai can be found online: https://www.lead-dbs.org/helpsupport/knowledge-base/videos/). Moreover, the novice raters localized 28 subthalamic DBS-electrodes from 7 PD-patients that received both post-operative MRI and CT under supervision of Lead-DBS programming team members, i.e. with the possibility to ask questions if in doubt. Finally, all 6 raters, independently and without any supervision or exchange, localized a set of 52 subthalamic DBS-electrodes of 13 PD-patients using either post-operative MRI or CT. Each DBS-electrode was thus localized twice in a randomized and blind order, to avoid any inference from one imaging modality to the other that was analyzed in the following.

Except for the expert rater, the remaining 5 raters were considered as "non-experts" and grouped as such. Electrode localization was performed with Lead-DBS software (www.lead-dbs.org; Horn & Kühn, 2015b) using the default work-flow of version 2.1.7 as described in Horn et al. (2019a). Specifically, pre- and postoperative imaging were linearly co-registered, refined using the 'brain shift correction' module in Lead-DBS (Horn et al., 2019b) and normalized into MNI-space using the effective: low variance + subcortical refinement preset (Ewert et al., 2019) for advanced normalization tools (Avants et al., 2008). Electrode trajectories were automatically pre-localized using Lead-DBS but had to be manually refined in most cases by mid-centering an electrode model in the antero-posterior, dorso-ventral and medio-lateral axis. The placement had to be judged by each rater individually, which can introduce variance as the postoperative artifact is larger than the actual electrode, presents with blurred borders that are specifically pronounced on the tip of the electrode, and visual landmarks of electrode contacts are reflected in varying artifact contrast intensity that must be recognized correctly (see Fig. 1).

Statistical analyses

As measure of variance, the Euclidean distance was computed between the localized DBS contacts by one rater versus each other rater. This was done for the x-, y- and z- coordinates separately as well as for the overall distance across axes. Distances were averaged across all possible pairs of raters and between the four DBS contact locations in either i) native or ii) ICBM 2009b NLIN ASym ('MNI') space, all possible pairs and within the same post-operative imaging modality. In a first step, this value was computed separately across non-expert raters and from non-expert raters to the expert rater. In the following analyses, localizations of all raters were considered. Paired permutation tests were carried out when testing for differences in distance, depending on raters' expertise, space or post-operative modality.

Results

Variance in electrode location similar across expert and non-expert raters in most axes

When considering distances of electrode locations in native space from post-operative CT and MRI imaging combined, the overall distance between expert and non-expert raters was not significantly different to that across non-expert raters (Non-Experts To Non-Experts: 0.57 ± 0.2 mm; Non-Experts To Expert: 0.53 ± 0.1 mm; P-Val>0.05, see Fig. 2A). Considering the three Cartesian axes separately, the distance along the z-axis increased on average by 0.04 mm between pairs of non-expert raters than to the expert rater (Non-Experts to Non-Experts: 0.36 ± 0.1 mm; Non-Experts to Experts: 0.32 ± 0.1 mm; P-Val=0.02).

Variance in electrode location is similar across post-operative imaging modalities

When comparing distances across all raters in native space, there was no significant difference in overall distance between the post-operative imaging modality used (CT=0.52 ± 0.2 mm; MRI=0.6 ± 0.3 mm; $P = 0.08$), see Fig. 2B. When considering Cartesian axes separately, variance in the x- and y-axes increased by 0.07 mm and 0.11 mm respectively when post-operative MRI was used (X-Axis: CT=0.19 ± 0.1 mm, MRI=0.26 ± 0.2, $P = 0.002$; Y-Axis: CT=0.22 ± 0.1 mm; MRI=0.33 ± 0.2 mm; $P = 0.001$).

Normalization to standard space increases the variance in DBS-location by <0.2 mm

Both the overall distance as well as the distance calculated for each axis separately was larger after normalization to MNI- than in native patient space. The average difference ranged between 0.02 – 0.15 mm, see Fig. 2C. When averaged across axes and post-operative imaging modalities, the average distance in MNI-space was 0.72 ± 0.25 mm and 0.57 ± 0.2 mm in native space ($P<0.001$).

Closest contact to "sweet spot" is stable against localization variance

Although normalization increased variance in DBS-electrode location, the contact closest to the optimal stimulation site ("sweet spot") of subthalamic DBS in PD as identified by Caire et al. (2013) showed strong overlap across raters. When post-operative MRI was used, the same contact resided closest to the sweet spot across raters in 94.8% ($n = 148$ of 156). In the remaining 8 cases, the closest contact was mostly one contact above ($n = 4$) or below ($n = 3$). When post-operative CT was used for co-registration, the closest contact overlapped in 87.1% ($n = 136$ of 156) of cases with all other cases being either one contact above ($n = 15$) or below ($n = 5$) the majority, see Fig. 2D.

Discussion

In the present study, we investigated the variance in location of subthalamic DBS-electrodes when using the widely used and freely available open-source software toolbox Lead-DBS. We show that across raters, modalities, and both in native and standard space, interrater variance in electrode location remains below the image resolution of 1 mm. The most robust results were obtained with post-operative CT in native space, where the interrater variance was 0.5 mm across axes, see Fig. 3, and the variance increased by 0.3 mm in the conditions with highest variance in our study – i.e. using post-operative MRI or normalizing to MNI-space.

However, these results may have been impacted by the currently used MRI sequences as these have an impact on the nature of the artifact resulting from the indwelling hardware. For instance, sequences with T2 weighting have been reported to produce more florid artifacts

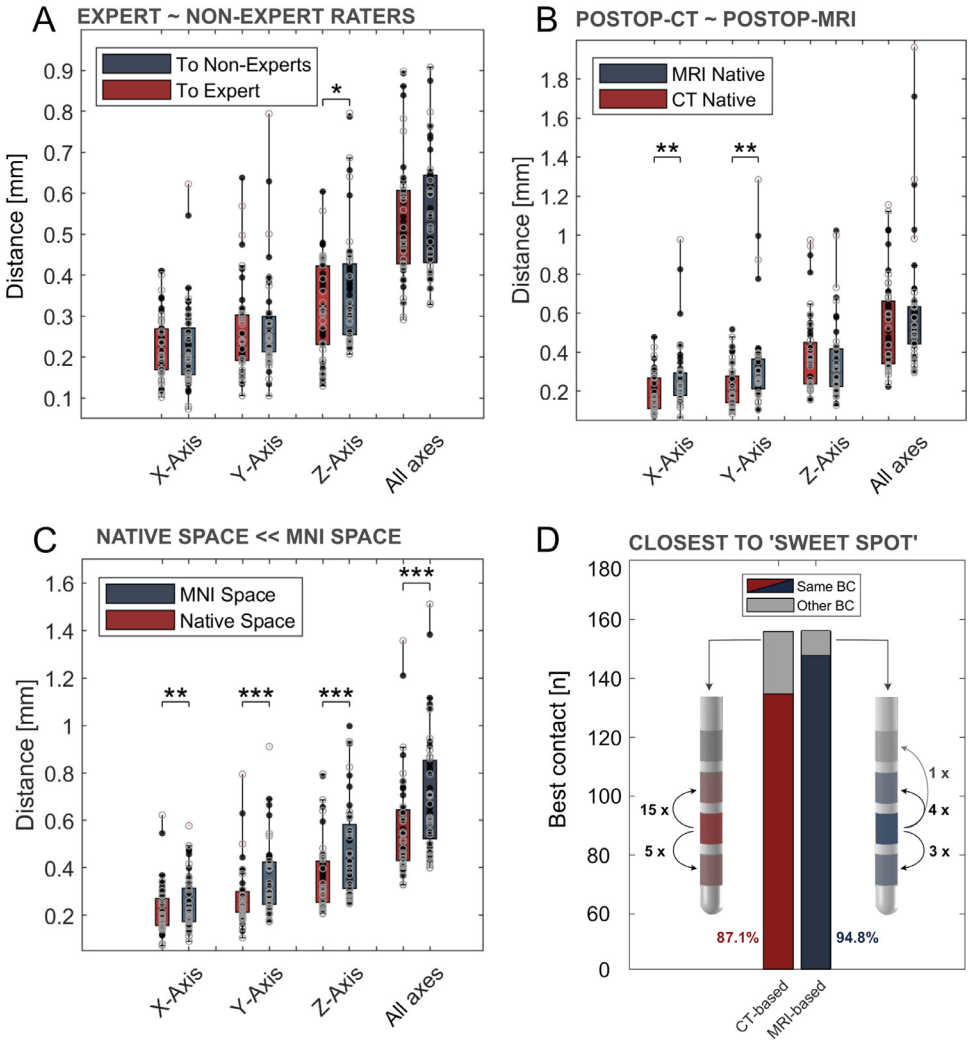

Fig. 2. Similar variance in DBS-localization across raters, modalities, and spaces. (A) When comparing distance in electrode localization across pairs of non-expert raters (blue box plots) with the ones between non-experts and an expert rater (red box plots), independently of post-operative imaging modality and separately for lower- (dark gray dots) and uppermost (light gray dots) contacts, there was no significant difference in overall distance across axes. Only along the z-axis, non-expert raters showed an increase of 0.04 mm among each other when compared to the expert rater. **(B)** When comparing the distance between electrode localization between post-operative imaging modalities, there was no significant difference in overall distance between MRI (blue boxplots) and CT (red boxplots) in native space – although distances were larger along the x- (0.07 mm) and y-axes (0.11 mm) when relying on post-operative MRI. **(C)** With normalization, an increase of 0.02–0.15 mm variance in DBS-localization was observed across axes. **(D)** When compared to the majority of raters, the rater-dependent localization led to a different choice in the optimal contact ('best contact', defined as contact closest to the "sweet spot" of STN-DBS) in 5.2% using post-operative MRI (blue) and 12.9% using post-operative CT (red). Note that outliers (defined as cases with interrater distance >3 standard deviations from the mean in the respective condition) all relied on the dorso-ventral misplacement of the right electrode of subject 6 by one rater (Fig. S1). In all boxplots, central marks indicate the median and edges the 25th and 75th percentiles of the distribution. $^{*}p<0.05$, $^{**}p<0.01$, $^{***}p<0.001$.

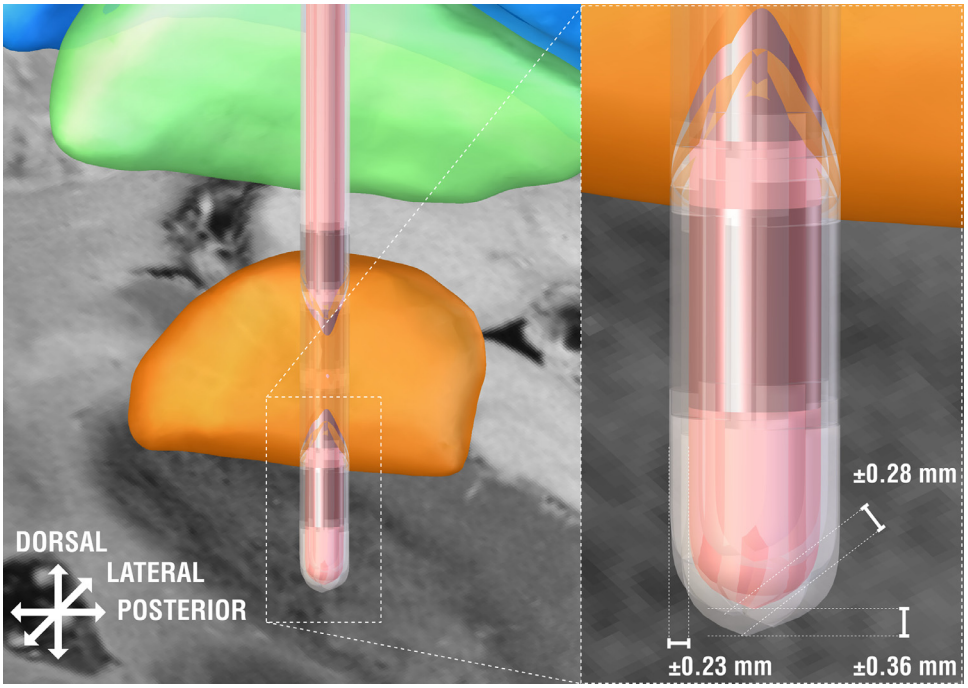

Fig. 3. Exemplary case of shift in DBS-electrode localization induced by different raters. The right DBS-electrode of example subject 9 is shown as localized by a single rater (red). The electrode was shifted in space (light gray versions) by the average interrater variance per axis in native space when averaged across post-operative neuroimaging modalities (antero-posterior shift of ±0.23 mm, ventro-dorsal shift of ±0.36 mm and medio-lateral shift of ±0.28 mm).

due to susceptibility effects (Martinez-Santiesteban et al., 2007). Furthermore, different lead types (segmented vs. omnidirectional) will produce differently shaped artifacts on both CT and MRI (Dembek et al., 2017; Husch et al., 2018; Sitz et al., 2017) while not all models have yet been approved for postoperative MRIs. Finally, DBS lead extensions (often forming a loop) placed around the burr hole device before connecting to extension cables can produce a 'chocking' effect again reducing the artifact at the tip of the lead (In et al., 2017). Beyond phantom studies, Hyam et al., 2015 have shown that the MRI artifact represents the actual tract in the brain after lead removal, which could be used to further confirm lead placement results on MRI.

Importantly, we showed that even after normalization and when using post-operative MRI for electrode localization, closest contact to the clinical "sweet spot" of subthalamic DBS (Caire et al., 2013) remained stable in the majority of cases (87–95%). Taken together, we consider that variance introduced by raters in DBS-electrode location is reasonably low when using Lead-DBS, independently of the post-operative imaging modality used and even for newly trained but fairly unexperienced users. These findings are crucial to better judge scientific results provided by analyses with Lead-DBS and close a missing link in the processing pipeline that had thus far not been objectively assessed.

Funding

Roxanne Lofredi and Leon A. Steiner are participants in the BIH Charité (Junior) Clinician Scientist Program funded by the Charité – Universitätsmedizin Berlin, and the Berlin Institute of Health at Charité (BIH). The work was supported by Deutsche Forschungsgemeinschaft (Project-ID 424,778,381 – TRR 295 Retune). This is an EU Joint Program – Neurodegenerative Disease (JPND) project. The project is supported through the following funding organisations under the aegis of JPND - www.jpnd.eu (A.H.: the Deutsches Zentrum für Luft- und Raumfahrt - Germany; B.C.M.v.W.: the Netherlands organisation for Health Research and Development (ZonMw) - The Netherlands). A.H. was additionally supported by the German Research Foundation (Deutsche Forschungsgemeinschaft, Emmy Noether Stipend 410,169,619 and 424,778,381 – TRR 295), the Foundation for OCD research (FFOR) and the NIH (2R01 MH113929).

Data availability statement

The underlying raw data to this manuscript (patient MRI and post-operative CTs) cannot be openly shared because it contains sensible patient-identifiable information. All code used to analyze data as presented in the manuscript is openly available within the Lead-DBS software (https://github.com/netstim/leaddbs; https://www.lead-dbs.org/).

Declaration of competing interests

The authors declare that they have no known competing financial interests or personal relationships that could have appeared to influence the work reported in this paper

Credit authorship contribution statement

Roxanne Lofredi: Conceptualization, Formal analysis, Investigation, Methodology, Validation, Visualization, Writing – original draft. **Cem-Georg Auernig:** Data curation, Formal analysis, Investigation, Writing – review & editing. **Siobhan Ewert:** Data curation, Investigation, Methodology, Project administration, Writing – review & editing. **Friederike Irmen:** Data curation, Investigation, Methodology, Project administration, Writing – review & editing. **Leon A. Steiner:** Investigation, Methodology, Writing – review & editing. **Ute Scheller:** Investigation, Methodology, Writing – review & editing. **Bernadette C.M. van Wijk:** Investigation, Methodology, Writing – review & editing. **Simon Oxenford:** Resources, Software, Writing – review & editing. **Andrea A. Kühn:** Funding acquisition, Resources. **Andreas Horn:** Funding acquisition, Project administration, Supervision, Writing – review & editing.

Data Availability

The data that has been used is confidential.

Supplementary materials

Supplementary material associated with this article can be found, in the online version, at doi:10.1016/j.neuroimage.2022.119552.

References

Alkemade, A., Groot, J.M., Forstmann, B.U., 2018. Do we need a human post mortem whole-brain anatomical ground truth in in vivo magnetic resonance imaging? Front. Neuroanat. 12, 110. https://www.frontiersin.org/article/10.3389/fnana.2018.00110.

Avants, B.B., Epstein, C.L., Grossman, M., Gee, J.C., 2008. Symmetric diffeomorphic image registration with cross-correlation: evaluating automated labeling of elderly and neurodegenerative brain. Med. Image. Anal. 12 (1), 26–41. doi:10.1016/j.media.2007.06.004.

Caire, F., Ranoux, D., Guehl, D., Burbaud, P., Cuny, E., 2013. A systematic review of studies on anatomical position of electrode contacts used for chronic subthalamic stimulation in Parkinson's disease. Acta Neurochir. (Wien.) 155 (9), 1647–1654. doi:10.1007/s00701-013-1782-1, discussion 1654.

Dembek, T.A., Hoevels, M., Hellerbach, A., Horn, A., Petry-Schmelzer, J.N., Borggrefe, J., Wirths, J., Dafsari, H.S., Barbe, M.T., Visser-Vandewalle, V., Treuer, H., 2019. Directional DBS leads show large deviations from their intended implantation orientation. Parkinsonism Relat. Disord. 67, 117–121. doi:10.1016/j.parkreldis.2019.08.017.

Dembek, Till A., Reker, P., Visser-Vandewalle, V., Wirths, J., Treuer, H., Klehr, M., Roediger, J., Dafsari, H.S., Barbe, M.T., Timmermann, L., 2017. Directional DBS increases side-effect thresholds—a prospective, double-blind trial. Mov. Disord. 32 (10), 1380–1388. doi:10.1002/mds.27093.

Edlow, B.L., Mareyam, A., Horn, A., Polimeni, J.R., Witzel, T., Tisdall, M.D., Augustinack, J.C., Stockmann, J.P., Diamond, B.R., Stevens, A., Tirrell, L.S., Folkerth, R.D., Wald, L.L., Fischl, B., & van der Kouwe, A. (2019). 7 Tesla MRI of the ex vivo human brain at 100 μm resolution. *Sci. Data*, 6(1), 244. https://doi.org/10.1038/s41597-019-0254-8

Ewert, S., Horn, A., Finkel, F., Li, N., Kühn, A.A., Herrington, T.M., 2019. Optimization and comparative evaluation of nonlinear deformation algorithms for atlas-based segmentation of DBS target nuclei. Neuroimage 184, 586–598. doi:10.1016/j.neuroimage.2018.09.061.

Ewert, S., Plettig, P., Li, N., Chakravarty, M.M., Collins, D.L., Herrington, T.M., Kuhn, A.A., Horn, A., 2018. Toward defining deep brain stimulation targets in MNI space: a subcortical atlas based on multimodal MRI, histology and structural connectivity. Neuroimage 170, 271–282. doi:10.1016/j.neuroimage.2017.05.015.

Horn, A., 2019. The impact of modern-day neuroimaging on the field of deep brain stimulation. Curr. Opin. Neurol. 32 (4), 511–520. doi:10.1097/WCO.0000000000000679.

Horn, A., Fox, M.D., 2020. Opportunities of connectomic neuromodulation. Neuroimage 221, 117180. doi:10.1016/j.neuroimage.2020.117180.

Horn, A., Kühn, A.A., 2015a. NeuroImage Lead-DBS : a toolbox for deep brain stimulation electrode localizations and visualizations. Neuroimage 107, 127–135. doi:10.1016/j.neuroimage.2014.12.002.

Horn, A., Kühn, A.A., 2015b. Lead-DBS: a toolbox for deep brain stimulation electrode localizations and visualizations. Neuroimage 107, 127–135. doi:10.1016/j.neuroimage.2014.12.002.

Horn, A., Kühn, A.A., Merkl, A., Shih, L., Alterman, R., Fox, M., 2017. Probabilistic conversion of neurosurgical DBS electrode coordinates into MNI space. Neuroimage 150, 395–404. doi:10.1016/j.neuroimage.2017.02.004.

Horn, A., Li, N., Dembek, T.A., Kappel, A., Boulay, C., Ewert, S., Tietze, A., Husch, A., Perera, T., Neumann, W.-.J., Reisert, M., Si, H., Oostenveld, R., Rorden, C., Yeh, F.-.C., Fang, Q., Herrington, T.M., Vorwerk, J., Kuhn, A.A., 2019a. Lead-DBS v2: towards a comprehensive pipeline for deep brain stimulation imaging. Neuroimage 184, 293–316. doi:10.1016/j.neuroimage.2018.08.068.

Horn, A., Wenzel, G., Irmen, F., Huebl, J., Li, N., Neumann, W.J., Krause, P., Bohner, G., Scheel, M., Kühn, A.A., 2019b. Deep brain stimulation induced normalization of the human functional connectome in Parkinson's disease. Brain 142 (10), 3129–3143. doi:10.1093/brain/awz239.

Husch, A., Petersen, V., Gemmar, M., Goncalves, P., Hertel, F, 2018. PaCER - a fully automated method for electrode trajectory and contact reconstruction in deep brain stimulation. NeuroImage: Clinical 17, 80–89. doi:10.1016/j.nicl.2017.10.004.

Hyam, J.A., Akram, H., Foltynie, T., Limousin, P., Hariz, M., Zrinzo, L., 2015. What You see is what you get: lead location within deep brain structures is accurately depicted by stereotactic magnetic resonance imaging. Neurosurgery 11 (3), 412–419. doi:10.1227/NEU.0000000000000848, Suppldiscussion 419.

In, M.-.H., Cho, S., Shu, Y., Min, H.-.K., Bernstein, M.A., Speck, O., Lee, K.H., Jo, H.J., 2017. Correction of metal-induced susceptibility artifacts for functional MRI during deep brain stimulation. Neuroimage 158, 26–36. doi:10.1016/j.neuroimage.2017.06.069.

Martinez-Santiesteban, F.M., Swanson, S.D., Noll, D.C., Anderson, D.J., 2007. Magnetic field perturbation of neural recording and stimulating microelectrodes. Phys. Med. Biol. 52 (8), 2073–2088. doi:10.1088/0031-9155/52/8/003.

Milchenko, M., Snyder, A.Z., Campbell, M.C., Dowling, J.L., Rich, K.M., Brier, L.M., Perlmutter, J.S., Norris, S.A., 2018. ESM-CT: a precise method for localization of DBS electrodes in CT images. J. Neurosci. Methods 308, 366–376. doi:10.1016/j.jneumeth.2018.09.009.

Oxenford, S., Roediger, J., Milosevic, L., Güttler, C., Spindler, P., Vajkoczy, P., Neumann, W.-J., Kühn, A., Horn, A., 2021. Lead-OR: a multimodal platform for deep brain stimulation surgery. MedRxiv doi:10.1101/2021.08.09.21261792, 2021.08.09.21261792.

Sitz, A., Hoevels, M., Hellerbach, A., Gierich, A., Luyken, K., Dembek, T.A., Klehr, M., Wirths, J., Visser-Vandewalle, V., Treuer, H., 2017. Determining the orientation angle of directional leads for deep brain stimulation using computed tomography and digital x-ray imaging: a phantom study. Med. Phys. 44 (9), 4463–4473. doi:10.1002/mp.12424.

Treu, S., Strange, B., Oxenford, S., Neumann, W.-J., Kühn, A., Li, N., Horn, A., 2020. Deep brain stimulation: imaging on a group level. Neuroimage 219, 117018. doi:10.1016/j.neuroimage.2020.117018.

Vogel, D., Shah, A., Coste, J., Lemaire, J.-J., Wårdell, K., Hemm, S., 2020. Anatomical brain structures normalization for deep brain stimulation in movement disorders. NeuroImage: Clinical 27, 102271. doi:10.1016/j.nicl.2020.102271.